



OPEN

Dysregulated Ca^{2+} Homeostasis in Fanconi anemia cells

SUBJECT AREAS:

ION CHANNELS

EXPERIMENTAL MODELS OF
DISEASECesare Usai¹, Silvia Ravera², Paola Cuccarolo³, Isabella Panfoli², Carlo Dufour⁴, Enrico Cappelli^{4*}
& Paolo Degan^{3*}Received
19 November 2014Accepted
15 December 2014Published
28 January 2015Correspondence and
requests for materials
should be addressed to
P.D. (paolo.degan@
hsanmartino.it)* These authors
contributed equally to
this work.

¹Institute of Biophysics, National Research Council, 16149 Genova, Italy, ²DIFAR-Biochemistry Lab., Department of Pharmacology, University of Genova, 16132 Genova, Italy, ³S. C. Mutagenesis, IRCCS AOU San Martino–IST (Istituto Nazionale per la Ricerca sul Cancro), CBA Torre A2, 16123 Genova, Italy, ⁴Hematology Unit, Istituto Giannina Gaslini, 16148 Genova, Italy.

Fanconi Anemia (FA) is a rare and complex inherited blood disorder associated with bone marrow failure and malignancies. Many alterations in FA physiology appear linked to red-ox unbalance including alterations in the morphology and structure of nuclei, intermediate filaments and mitochondria, defective respiration, reduced ATP production and altered ATP/AMP ratio. These defects are consistently associated with impaired oxygen metabolism indeed treatment with antioxidants N-acetylcysteine (NAC) and resveratrol (RV) does rescue FA physiology. Due to the importance of the intracellular calcium signaling and its key function in the control of intracellular functions we were interested to study calcium homeostasis in FA. We found that FANCA cells display a dramatically low intracellular calcium concentration ($[\text{Ca}^{2+}]_i$) in resting conditions. This condition affects cellular responses to stress. The flux of Ca^{2+} mobilized by H_2O_2 from internal stores is significantly lower in FANCA cells in comparison to controls. The low basal $[\text{Ca}^{2+}]_i$ in FANCA appears to be an actively maintained process controlled by a finely tuned interplay between different intracellular Ca^{2+} stores. The defects associated with the altered Ca^{2+} homeostasis appear consistently overlapping those related to the unbalanced oxidative metabolism in FA cells underlining a contiguity between oxidative stress and calcium homeostasis.

FA is a rare and complex inherited blood disorder of the child. As much as at least 16 genes are associated with the disease. The highest mutations frequency occurs among three genes (FANCA, FANCC and FANCG). Likely FA proteins play important roles in the maintenance of hematopoiesis since the disease is linked with hematopoietic dysfunctions and pathologies. In FA patients high apoptosis rates and reduced growth ability may result in the development of anemia, neutropenia, thrombocytopenia and bone marrow (BM) failure¹. Elevated basal oxidative stress, DNA repair defects, altered expression of TNF-alpha and other cytokines²⁻³ are recognized hallmarks of the FA phenotype⁴. The combination of genetic instability and cytokine hypersensitivity creates an environment supporting the selection of malignant leukemic clones. 20–25% of FA patients develop malignancies of myeloid origin, including acute myeloid leukemia (36%; 600-fold increased risk), myelodysplastic syndrome (54%; 5000-fold increased risk) and solid tumors⁵. The majority of the phenotype-related manifestations in FA can be linked to red-ox alteration. FA cells display altered morphology, at nuclei, mitochondria and subcellular reticula, altered expression and processing of selected structural proteins and defects in the respiratory and energy metabolism^{6,7}.

Ca^{2+} ions acts as regulators in almost all physiological processes in cells and organisms, in signal transduction and as second messengers and any disturbance in the mechanisms involved in the control of the intracellular Ca^{2+} concentration ($[\text{Ca}^{2+}]_i$) are associated with multiple pathological processes⁸. Because of the crucial role of Ca^{2+} homeostasis in cellular physiology and, as far as we know, of the unavailability of these information in FA, this issue needed to be explored. The resting $[\text{Ca}^{2+}]_i$ in the cytoplasm is normally maintained in the nano-molar range, roughly between 50–100 nM. Signals occurs when cells are stimulated to release Ca^{2+} ions from intracellular stores, and/or when Ca^{2+} enters in the cells through membrane ion channels. Specific signals can trigger a sudden increase in $[\text{Ca}^{2+}]_i$ level up to 500–1,000 nM by the opening of the channels in the endoplasmic reticulum (ER), mitochondria or in the plasma membrane. ER is the major Ca^{2+} store but a crucial role of mitochondria in Ca^{2+} signaling has also been recently established⁹. Mitochondrial Ca^{2+} concentration $[\text{Ca}^{2+}]_m$ responds to rapid changes in cytosolic Ca^{2+} through the Ca^{2+} uniporter system¹⁰. Mitochondrial membrane depolarization and inhibition of the electron transport chain or suppression of Ca^{2+} uptake prevents Ca^{2+} influx¹¹. Conversely Ca^{2+} influx in mitochondria can be increased by inhibiting the SERCA channels in the ER with thapsigargin¹².



Therefore Ca^{2+} signaling appears to be maintained through a finely tuned dynamic interplay between endoplasmic reticulum, mitochondria, and plasma membrane¹³.

Ca^{2+} regulates many cellular ATP consuming reactions, and Ca^{2+} appear as a crucial signaling molecule in the energy metabolism¹⁴. Ca^{2+} uptake into mitochondria activates the tri-carboxylic acid (TCA) cycle which supply NADH for the oxidative phosphorylation. Electron transfer coupled with proton pumping in the inter-mitochondrial membrane space establish the electrochemical potential used to convert ADP to ATP¹⁵. Mitochondria however are also the most important source of free radical production and have a crucial role in the cytotoxic $[\text{Ca}^{2+}]_i$ and the consequent negative effects associated with the induction of intrinsic cell death^{16,17}.

We recently characterized a number of defects in FA strictly associated with an altered mitochondrial physiology. In this study we explored Ca^{2+} homeostasis in FA cells from three different complementation groups. We also characterized $[\text{Ca}^{2+}]_i$ by red-ox modulation with the final aim to gather information of possible therapeutic benefits.

Results

Low basal $[\text{Ca}^{2+}]_i$ in FANCA cells. In a first series of experiments $[\text{Ca}^{2+}]_i$ was measured in FANCA, FANCA-corr and wt fibroblasts under basal, unstressed conditions. As reported in Table 1, in wt basal $[\text{Ca}^{2+}]_i$ was 64 ± 4 nM. In FANCA-corr cells $[\text{Ca}^{2+}]_i$ was comparable (62 ± 4 nM) to the value measured in wt cells whereas in FANCA cells $[\text{Ca}^{2+}]_i$ was 23 ± 3 nM, almost three folds lower. There was no significant difference in the measure of the basal $[\text{Ca}^{2+}]_i$ levels either in PBS buffer or in Ca^{2+} -free buffer (PBS, 0 Ca plus 2 mM EGTA). The same results were obtained employing FANCA lymphocytes (data not shown). Normal lymphocytes (wt) and FANCA-corr lymphoblast behave as the wt fibroblasts (data not shown). Table 1 reports also results concerning FANCC and FANCG fibroblast. Basal $[\text{Ca}^{2+}]_i$ levels was 24 ± 3 and 20 ± 5 for FANCC and FANCG cells, respectively, significantly similar to those measured in FANCA cells.

Treatment of cells with H_2O_2 . Cells were challenged with $100 \mu\text{M}$ H_2O_2 . This treatment resulted in a large increase in $[\text{Ca}^{2+}]_i$ in FANCA as well as in wt and FANCA-corr cells (Tab. 1) however the extent of Ca^{2+} fluxes in FANCA and control cells was quite different. In FANCA cells challenge with H_2O_2 resulted in an increase of $[\text{Ca}^{2+}]_i$ from 23 ± 3 nM to 174 ± 22 nM while in wt and FANCA-corr cells the same H_2O_2 treatment results in the increase of $[\text{Ca}^{2+}]_i$ from 64 ± 4 to 331 ± 18 and from 62 ± 4 to 326 ± 12 respectively. Thus final $[\text{Ca}^{2+}]_i$ in FANCA remains dramatically and significantly lower (0.5 folds; 174 ± 22 nM in FANCA in comparison to 331 ± 18 and 326 ± 12 nM in wt and FANCA-corr cells, respectively) after H_2O_2 treatment. Measurements performed in Ca^{2+} -free buffer were closely alike. Basal $[\text{Ca}^{2+}]_i$ levels were 24 ± 3 and 20 ± 5 nM for FANCC and FANCG cells, respectively, significantly similar to the level measured

in FANCA cells. Upon challenge with H_2O_2 FANCG cells display an increase of $[\text{Ca}^{2+}]_i$ from 20 ± 5 to 167 ± 9 nM, in close agreement with the data obtained for FANCA cells. In FANCC cells H_2O_2 treatment resulted in an increase of $[\text{Ca}^{2+}]_i$ from 24 ± 3 to 243 ± 13 nM. Therefore H_2O_2 treatment induces in FANCC cells a $[\text{Ca}^{2+}]_i$ significantly higher with respect to FANCA or FANCG cells.

Confocal microscopy measurements. Rhod2-AM loaded cells were used to study the Ca^{2+} fluxes in cells treated with H_2O_2 . The fluorescent Ca^{2+} indicator Rhod2-AM accumulates in mitochondria in living cells²⁰. Indeed, co-staining of cells with both Rhod2-AM and the mitochondrial fluorescent marker DiOC6 showed the good colocalization of the two dyes (Fig. 1).

Fig. 2 reports Rhod2-AM fluorescence decrease upon treatment of both FANCA and control cells with H_2O_2 . Experimental data were fitted by a four parameter logistic curve, with constraints $\text{max} > \text{min}$, $\text{EC}_{50} > 0$, $\text{min} > 0$ $\text{max} = 1$. The kinetic of the fluorescence decrease was faster in FANCA ($\text{EC}_{50} = 77$, Hill slope -2) than in control cells ($\text{EC}_{50} = 82$, Hill slope -1.7). Similar results were obtained in PBS buffer (Fig. 2A) or in buffer without Ca^{2+} (PBS-no- Ca^{2+} plus EGTA; Fig. 2B) suggesting that the H_2O_2 -induced mitochondrial Ca^{2+} efflux is independent of extracellular Ca^{2+} . Data suggest that treatment with H_2O_2 can cause an impairment in oxidative phosphorylation (ox-phos).

Measurements of $[\text{Ca}^{2+}]_i$ after challenge with Thapsigargin. Depletion of Ca^{2+} from ER was accomplished by treatment of the cells with Tg ($3 \mu\text{M}$), an irreversible blocker of the ER Ca^{2+} ATPases (SERCA). Table 2 reports how chronic (8 hours) treatment with Thapsigargin results in basal $[\text{Ca}^{2+}]_i$ levels that are superimposable to those in untreated cells (see Table 1) in both FANCA and wt cells. Interestingly, H_2O_2 challenge in these conditions resulted in Ca^{2+} fluxes of the same extent as those observed in untreated cells. However, upon Tg-treatment, a larger amount of Ca^{2+} is released from wt than FANCA cells suggesting that H_2O_2 induces mitochondrial Ca^{2+} depletion. On the other hand acute treatment with Tg at the same final concentration induces an increase in $[\text{Ca}^{2+}]_i$ in FANCA as well in wt cells. However this increase is higher in FANCA than in wt cells suggesting the release of a larger amount of Ca^{2+} from FANCA ER in comparison to wt ER. Data for FANCA-corr cells, not shown, are as for wt. In conclusion experiments with Tg suggest that the low basal $[\text{Ca}^{2+}]_i$ in FANCA is an actively maintained process whose control is shared by a finely tuned interplay between different intracellular Ca^{2+} stores. This underscores how mitochondria are important partners for Ca^{2+} fluxes playing with the ER a primary role in Ca^{2+} homeostasis.

Chronic Treatment with antioxidants. $[\text{Ca}^{2+}]_i$ was restored after chronic treatment with NAC or RV (Table 3). Both molecules were added to the growth media for 72 hours. Such increase of $[\text{Ca}^{2+}]_i$ was seen in all the tested conditions.

Table 1 | Basal $[\text{Ca}^{2+}]_i$ measured in WT, FANCA, FANCC, FANCG and FANCA-corr fibroblasts. Calcium concentration is expressed as nano-moles (nM). $[\text{H}_2\text{O}_2]$ was $100 \mu\text{M}$. Measures were made in PBS buffer (Ca^{2+} buffer, indicated with a + in the table) and in PBS without Ca^{2+} (PBS-no- Ca^{2+} plus 2 mM EGTA, indicated with a - in the table)

	Ca^{2+} buffer	Basal (untreat cells)	H_2O_2
WT	+	64 ± 4	331 ± 18
	-	57 ± 4	324 ± 15
FANCA	+	23 ± 3	174 ± 22
	-	25 ± 4	206 ± 21
FANCA-corr	+	62 ± 4	326 ± 12
	-	58 ± 5	324 ± 7
FANCC	+	24 ± 3	243 ± 13
FANCG	+	20 ± 5	167 ± 9

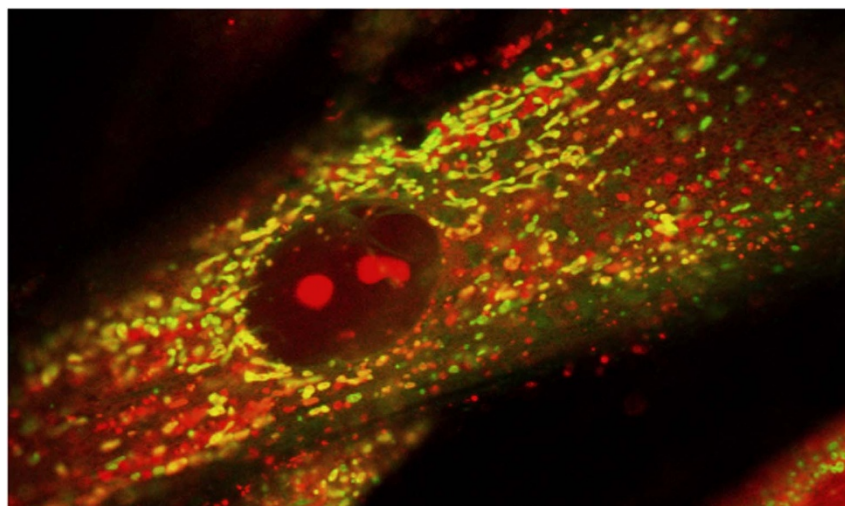


Figure 1 | Confocal microscopy image for the localization of DiOC6 and Rhod2-AM dyes in FANCA cells. Mitochondrial membranes were stained with 5 μM Rhod2-AM and 10 μM DiOC6 in PBS for 45 min at 37°C. Accumulation of Rhod2-AM and DiOC6 in mitochondria was followed by image microscopy. Figure shows the merge of the fluorescence signal from the two probes.

Ca²⁺-ATPase Activity. Untreated FANCA cells display a higher Ca²⁺-ATPase activity in comparison with wt and FANCA-corr cells (Fig. 3). Ca²⁺-ATPase activity can be associated with the ER SERCA pumps, considering that Tg inhibits the activity in all samples. This suggests that the activity of the pump efficiently removes the cytoplasmic Ca²⁺ and relocalizing it in the ER consistently to both the low level of [Ca²⁺]_i in FANCA cytoplasm and to the increased ER Ca²⁺ levels in comparison to controls. Moreover, the treatment with RV or NAC reduced the activity of Ca²⁺-ATPase activity at level similar to that observed in the control, confirming the data reported in Table 3.

Discussion

Our study reports the presence of an altered Ca²⁺ homeostasis in FA cells. Remarkably a dramatically low [Ca²⁺]_i level was measured in cells from three complementation groups of FA, FANCA, FANCC

and FANCG, which account for more than 90% of the FA patients. The low [Ca²⁺]_i level observed appear maintained by an active mechanism in cells in resting conditions as well as after exposure to H₂O₂. In fact in FANCA cells H₂O₂ increased [Ca²⁺]_i to 174 ± 22 nM while in wt and FANCA-corr cells [Ca²⁺]_i went up at 331 ± 18 and 326 ± 12, respectively (Table 1). This phenomenon appear mediated by an active ER-mediated calcium homeostasis. In FANCA ER appear overloaded with Ca²⁺, likely due to the higher Ca²⁺-ATPase activity observed in these cells in comparison with the controls. Indeed acute Tg treatment, which induced calcium release from ER, results in the enhanced release of calcium from FANCA in comparison with wt cells (Table 2). Conversely long-term Tg treatment (8 hours) does not modify the entity of calcium release observed when cells are exposed to H₂O₂ or to H₂O₂ plus Tg (Table 2).

Such low [Ca²⁺]_i condition in FA cells, while peculiar *per se*, has so far been reported to our best knowledge only in chronic myeloid

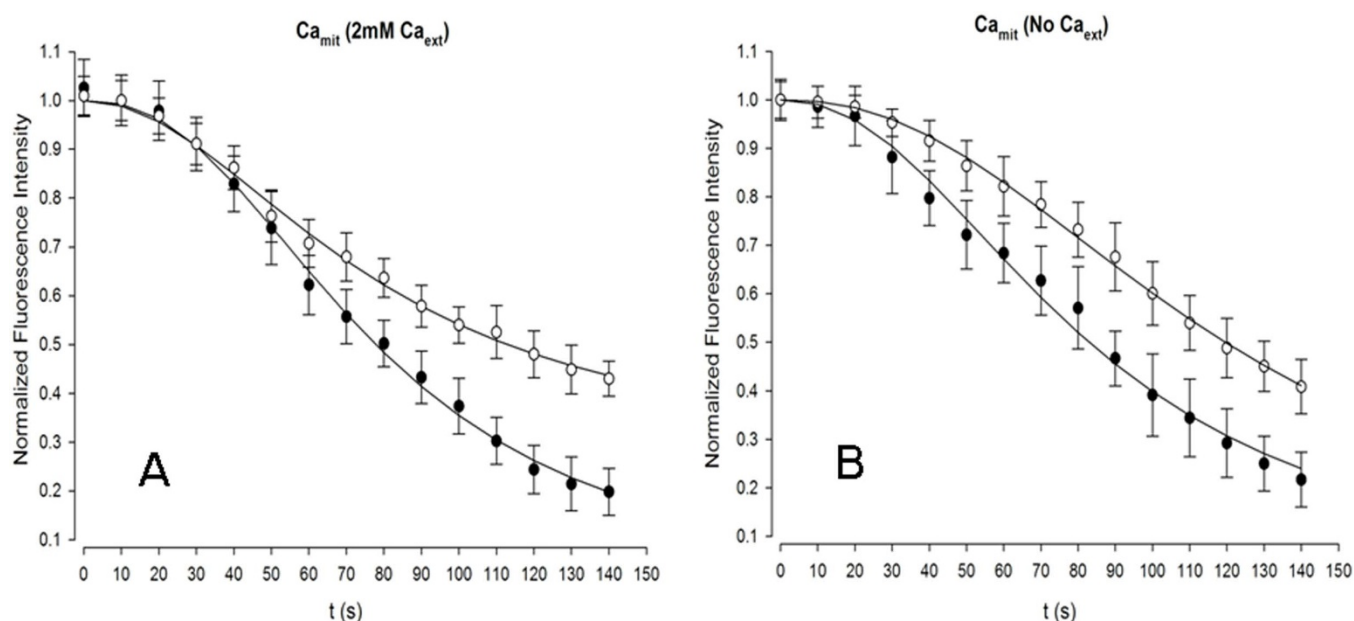


Figure 2 | Kinetic of Ca²⁺-depletion from mitochondria (Ca_{mit}) from cells stained with Rhod2-AM. Time (seconds) dependent fluorescence decrease is followed in Wt (open symbols) and FANCA (closed symbols) cells after treatment with 100 μM H₂O₂. A – data in Ca²⁺-containing buffer. B – data in buffer without Ca²⁺.



Table 2 | Thapsigargin-induced $[Ca^{2+}]_i$ fluxes. $[Ca^{2+}]_i$ was measured in wt and FANCA cells treated chronically (8 hours) with 3 μ M Tg (line 3). Tg treatment was followed by H_2O_2 (100 μ M) challenge (line 4). Acute Tg treatment (line 5) was accomplished in PBS buffer without Ca^{2+}

	WT	FANCA
Basal*	64 \pm 4	23 \pm 3
H_2O_2 *	331 \pm 18	174 \pm 22
Tg 8 h	55 \pm 4	28 \pm 2
Tg 8 h + H_2O_2	325 \pm 19	186 \pm 16
Tg (in no Ca^{2+})	195 \pm 11	326 \pm 23

*From Table 1.

leukemia (CML)^{21,22} and myeloid cells²³, which is interesting in the perspective of FA cancer proneness and the high prevalence in FA of malignancies of myeloid origin⁵. The low $[Ca^{2+}]_i$ may operate as a protective mechanism in delaying both cell cycle and DNA replication, thus allowing more time for DNA repair. Also, mitochondria appear involved in this tuning, consistently with the accepted role of mitochondria in shaping cytosolic Ca^{2+} signals and with the hypothesis that the mitochondrial Ca^{2+} buffering is relevant at discrete microdomains near the ER, where Ca^{2+} concentrations can reach high micromolar levels²⁴. Moreover, as mitochondrial TCA cycle dehydrogenases, as well as Pyruvate dehydrogenase phosphatase are the target for Ca^{2+} signaling within the mitochondrial matrix, any alteration in mitochondrial Ca^{2+} concentration impacts on the aerobic energy metabolism. In fact we have reported that FANCA cells display alterations in the aerobic mitochondrial respiration⁶.

It might be remarkable to note at this point that while basal $[Ca^{2+}]_i$ levels in FANCA, FANCC and FANCG cells are similar the response to a H_2O_2 challenge differs between FANCA and FANCG cells in comparison to FANCC. FANCA and FANCG display an analogous increase of $[Ca^{2+}]_i$ from 23 \pm 3 and 20 \pm 5 nM to 174 \pm 22 and 167 \pm 9 nM, respectively. IN FANCC cells H_2O_2 treatment induces an increase of $[Ca^{2+}]_i$ from 24 \pm 3 to 243 \pm 13 nM. Although still significantly lower than the value measured in wt and FANCA-corr cells the behavior of FANCC cells toward oxidative challenge might imply a significant difference in the Ca^{2+} homeostasis between these FA complementation groups. While this topic has potential interest at present the implications of this argument are difficult to assess.

In this study we report that a significantly lower Ca^{2+} efflux is recorded after an oxidative stress induced in FANCA cells. This Ca^{2+} flux results from mitochondrial Ca^{2+} stores depletion. The kinetic of this process is faster for FANCA cells in comparison with controls. Mitochondria are the core of cellular energy metabolism, being the site of ATP synthesis, which is modulated by Ca^{2+} homeostasis^{15,24,25}. Mitochondrial matrix Ca^{2+} overload can lead to enhanced reactive oxygen species (ROS) production triggering the onset of apoptotic cell death with the activation of the permeability transition pore, the cytochrome c release, PARP and caspase 9 activation through apoptosome formation. Indeed while FA cells display an enhanced basal level of apoptosis, intrinsic apoptosis is abnormal in FA. Several authors focused on different aspects of this problem,

Table 3 | Effects of NAC and Resveratrol in $[Ca^{2+}]_i$. FANCA and wt cells were treated with NAC (500 μ M) or RV (10 μ M) for 72 hours

	wt	FANCA
NAC	62 \pm 5	57 \pm 3
NAC + H_2O_2	325 \pm 18	330 \pm 19
RV	61 \pm 4	59 \pm 4
RV + H_2O_2	295 \pm 21	345 \pm 22

and the functional compromising of the mitochondria themselves has been recently addressed^{16,7,26,27}. We support the view that low $[Ca^{2+}]_i$ could limit mitochondria-driven apoptotic cell death in FA, in line with repeated observations focused on the peculiar unfolding of the FA apoptotic processing in association with defined defects in mitochondria functionality²⁸.

We have recently reported that FA physiology is thoroughly altered at the functional, molecular and structural level^{16,7,27,29,30}. Altered nuclei, mitochondria, ER and intermediate filaments morphology are associated with defective maturation and processing of structural proteins (mitofilin, vimentin, lamin) involved in their organization^{7,29}. Moreover, the molecular functions and the biochemical functionality of these subcellular domains are also affected. Altogether these alterations result in a new balance of the basal cellular metabolism that, until a certain point, appears still compatible with life²⁹. In this perspective the low $[Ca^{2+}]_i$ in FANCA cells may be regarded as an aspect of this unique condition. Then the question may be: which mechanism does allow the induction and maintenance of low $[Ca^{2+}]_i$? Primary contributors to this conditions are channels, transporters, pumps and binding proteins located primarily in the plasma membrane and inside those subcellular domains involved in the active operations of Ca^{2+} storage and disposal in response to defined physiological signals, i.e.: mitochondria and ER.

The mitochondrial population of FANCA cells displays significant abnormalities⁷. Mitofilin, a protein of the mitochondrial inner membrane involved in cristae formation and in protein trafficking is expressed with an altered molecular weight, as an immature precursor. Also the mitochondria reticulum in FANCA cells appears dispersed and fragmented in comparison to control cells. Mitochondria themselves appear dysmorphic. A similar cellular phenotype was observed in cells with mutations in OPA1. OPA1 is a dynamin-related GTPase protein anchored in the mitochondrial inner membrane and involved in mitochondrial fusion functions and membrane remodeling and responsible for dominant optic atrophy (DOA), the most common hereditary form of optic neuropathy. OPA1 loss has a role in dissipation of mitochondrial membrane potential and mitochondrial network fragmentation³¹. The correctness of the mitochondrial fusion and fission processes has emerged as a critical factor in the regulation of the mitochondrial pool and associated with the exclusion of respiration- and electrochemically incompetent organelles through autophagy³².

Bioenergetics defects in FANCA as well as in OPA1 defective cells are also associated with a decrease in the efficacy of NAD to NADH reduction which depletes mitochondria of NADH to fuel ox-phos at Complex I. OPA1-defective cells display significant mitochondrial Ca^{2+} overload which induces mitochondrial membrane permeability transition pore opening and depolarization which results in enhancement of apoptotic cell death³³.

Defects associated with loss or mutations in OPA1 gene makes us wonder what could be the function associated with FANCA. The possible absence of OPA1 is linked to a plethora of defects. Unfortunately the question is still open. However all these arguments might not be so farfetched (in consideration)/(with respect) that activity of OPA1 is essentially regulated by its association with the activity of a novel zinc metalloproteinase called OMA1 and identified as the essential membrane-polarization-sensitive protease for OPA1^{34,35}. OPA1-OMA1 interplay needs the maintenance of an efficient ox-phos and an appropriate Ca^{2+} load³⁶. All these alterations suggest that the normal mitochondrial turn-over is altered by an underlying stress condition. In FA the underlying stress might likely be associated with the altered red-ox metabolism which does affect mitochondrial morphology, functionality and protein maturation. We indeed reported in FANCA cells a defective activity of metalloproteinase²⁹. In conclusion data reported here support the idea that altered mitochondrial functionality in FA might be associated with the altered Ca^{2+} homeostasis.

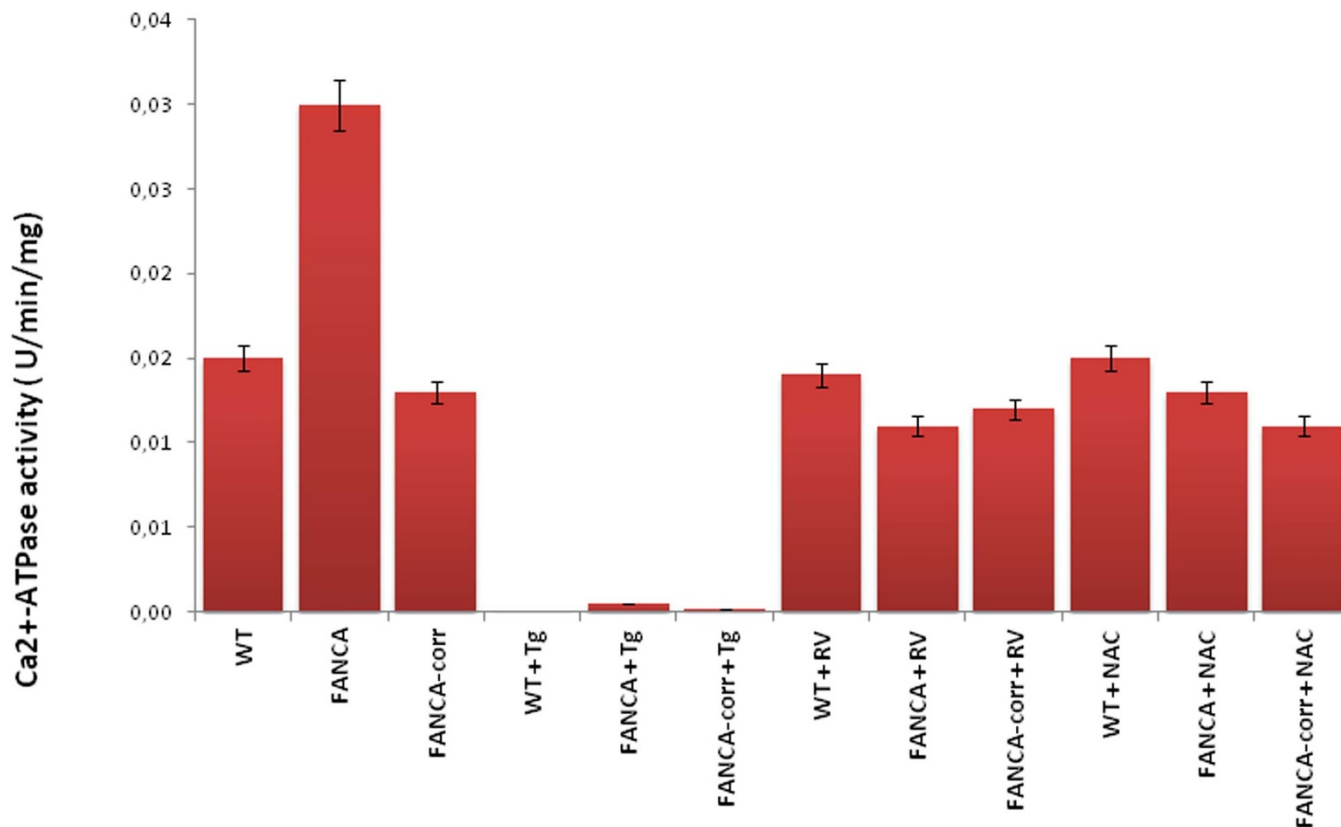


Figure 3 | Ca²⁺-ATPase activity. The graph reported the Ca²⁺-ATPase activity in FANCA FANCA-corr and wt cells. The activity was observed in the presence of Thapsigargin or in cells treated with RV or NAC. The activity is expressed as U/min/mg, calculated as $\mu\text{mol ATP hydrolyzed}/\text{min}/\text{mg}$. Each column is representative of at least four experiments and represent the mean \pm S.D.

Concerning the ER we reported⁷ how GRP94, a chaperonin localized in ER and involved in the folding and assembly of secreted and membrane-associated proteins is over-expressed in FANCA cells. Immunofluorescence studies also demonstrated for GRP94 in FANCA cells a different cellular localization in comparison to normal cells with protein staining coating cell nuclei and ER membranes extending from the outer nuclear membrane. GRP94, an homolog of HSP90, signals alterations of Ca²⁺ balance inside ER, redox status and protein glycosylation and is involved in the ER stress response and the unfolded protein response (UPR) whose purpose is to either restore homeostasis or target cell to apoptosis³⁷.

Data concerning GRP94 overexpression, activity of SERCA and the response of cells to thapsigargin do support the existence of FANCA alterations in ER Ca²⁺ homeostasis, in association with decreased mitochondrial Ca²⁺ buffering and decreased mitochondrial membrane potential. This scenario is suggestive of an altered communication between the two organelles^{38,39}. Key partners in this signaling process are proteins of the Bcl-2 family. One of the main functions of the Bcl-2 family is the control of Ca²⁺ homeostasis⁴⁰. GRP94 is implicated in these signaling activities since it acts in association with elements of the Bcl-2 family. Several Bcl-2 family members are involved in controlling apoptosis by modulation of the caspase activity and most of them are also located as multi-protein complexes at ER membranes. Stress signals associated with Ca²⁺ and ROS appear to travel from ER to mitochondria⁴¹. Several members of the Bcl-2 family interact with cellular Ca²⁺ signaling systems at many levels, in a complex web of potential interactions. Key interactions occur between Bcl-2-related proteins and IP3R. While there is still a lack of consensus concerning these interactions, a growing body of evidence supports models by which these interactions are tightly modulated⁴² also in consequence of a red-ox distress which affects mitochondria and ER communications⁴³.

It is interesting to note, finally, how in wild-type PLB-985 cells, a human diploid myeloid leukemia cell line, the high level of superoxide ions (O₂⁻) production was associated with a significant decrease in the membrane potential which, in turn, was addressed as a cause for the inhibition of the capacitative Ca²⁺ entry, which prevented [Ca²⁺]_i overload²³. In these cells the high O₂⁻ production was attributed to an increased activity of NADPH oxidase (NOX2)⁴⁴. Interestingly NADPH oxidase activity can in turn be stimulated by TNF- α ⁴⁵, which is typically elevated in FA. Conversely TNF- α is also involved in G-protein-coupled signal transduction which, through IP3, is involved in the modulation of the Ca²⁺ signals^{46,47}.

Concerning antioxidant treatment, both NAC and RV resulted in recovery of normal [Ca²⁺]_i. Also, both antioxidants normalize Ca²⁺ ATPase activity. Conceivably, the two molecules realize normalization of the [Ca²⁺]_i through different mechanisms²⁷. NAC essentially acts as a true antioxidant limiting ROS induction acting at the level of the mitochondrial Complex I activity⁶ and boosts mitochondrial oxidative metabolism finally accomplishing a direct effect on red-ox balance and an indirect effect on Ca²⁺ homeostasis. On the contrary RV, which is a direct mediator of intracellular Ca²⁺ signaling⁴⁸ in line with its activity as a sirtuin modulator⁴⁹ inhibits SERCA⁵⁰ and strongly affects mitochondrial functions including inhibition of ATP synthase⁵¹. Notably the recovery of a normal [Ca²⁺]_i is obtained with restoration of a normal red-ox balance.

In conclusion it appears that the defects attributed to altered Ca²⁺ homeostasis are consistently overlapping those related to alterations of the oxidative metabolism in FA cells. Indeed the abnormal manipulation of these signals results in diffuse defects which affects FA cells phenotype as a whole (Fig. 4). The peculiar Ca²⁺ signaling represents a distinctive trait that may be of value in the perspective of the knowledge of the biochemical mechanisms of FA with the final aim of possible therapeutic intervention.

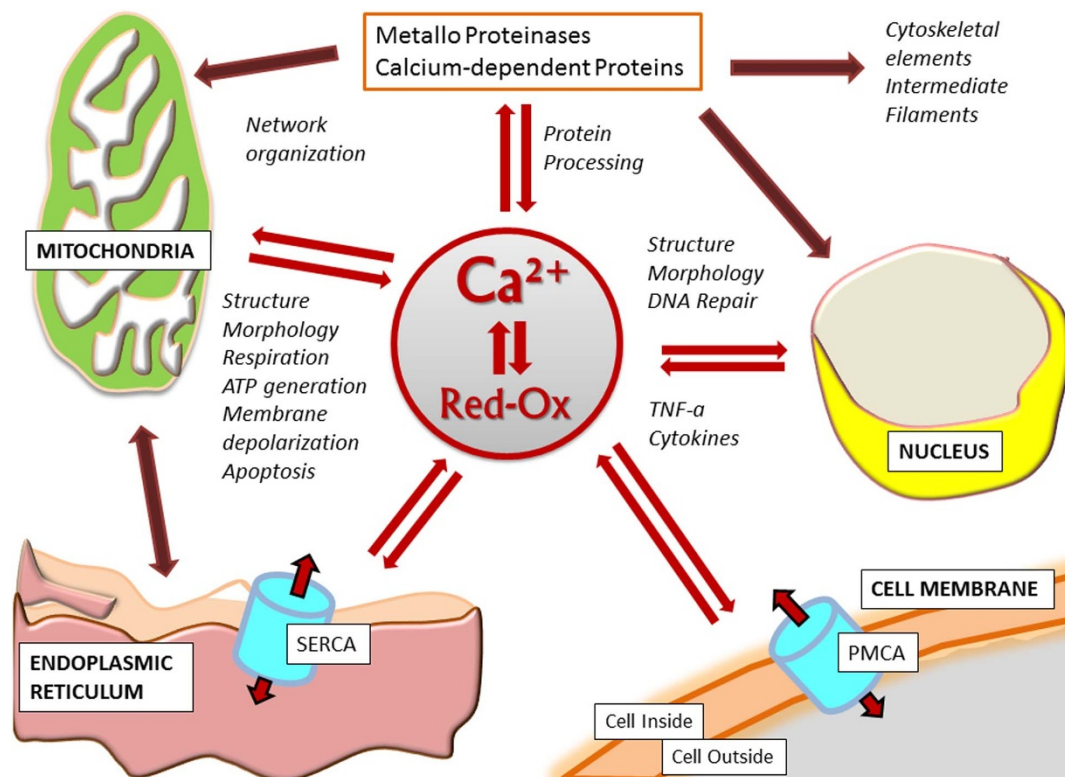


Figure 4 | Schematic representation of the functions and relationships that appear affected by the abnormal $[Ca^{2+}]$ and Red-Ox signaling in FANCA cells. Functions directly affected by the altered calcium signaling are indicated by the red double arrows. Following alteration of these primary targets other internal relationships, indicated by the dark red arrows, may result modified.

Methods

Cells. FANCA, FANCC and FANCG primary fibroblast cell lines, isogenic FANCA primary fibroblasts corrected with S11FAIN⁶ retrovirus and wild type (wt) cells were grown as monolayer at 37°C in RPMI supplemented with 10% fetal calf serum. FANCA, corrected FANCA (FANCA-corr) and wt lymphoblast and FANCA primary lymphocytes were also employed, as reported⁶, and were grown at 37°C in RPMI supplemented with 10% fetal calf serum and antibiotics. Primary normal and FA lymphocytes were isolated using Ficoll-Paque Plus and grown at 37°C in RPMI supplemented with 10% fetal calf serum, antibiotics and phytohemagglutinin (20 μ g/ml). N-acetylcysteine (NAC, 500 μ M), and resveratrol (RV, 10 μ M) were supplemented directly to the culture media once a day for 72 hours. H_2O_2 (100 μ M) and Thapsigargin (Tg, 3 μ M) were added directly to the cells in PBS buffer. All chemicals used were from Sigma-Aldrich (Italy) unless differently specified.

Fluorimetric Determination. $[Ca^{2+}]_i$ was measured by using the ratiometric membrane-permeant fluorescent indicator dye Fura2/AM (Invitrogen, Life Technologies, Italy). Cells grown on a 20 mm coverslips were incubated with 10 μ M Fura2/AM in standard PBS buffer for 45 min at 37°C and then washed at room temperature. Mitochondrial membranes were stained with 5 μ M Rhod2-AM (Invitrogen) and/or 10 μ M DiOC6 (Invitrogen) in PBS for 30 to 45 min at 37°C. Cells were then washed at room temperature.

Calculation of Cytosolic $[Ca^{2+}]_i$ Concentration. The intracellular free Ca^{2+} concentration was calculated according to following equation: $[Ca^{2+}]_i = \beta K_d (R - R_{min}) / (R_{max} - R)^{18}$ where R is E_{340}/E_{380} ; R_{min} is E_{340}/E_{380} in zero Ca^{2+} ; R_{max} is E_{340}/E_{380} in Ca^{2+} -saturated solution; β is E_{380} in zero Ca^{2+}/E_{380} in Ca^{2+} saturated solution and K_d is the dissociation constant of the dye at room temperature (140 nM). To obtain the R_{min} and R_{max} values, the Ca^{2+} ionophore ionomycin (2 nM) was added after each experiment in a zero- Ca^{2+} bath (0 Ca^{2+} , 2mM EGTA) and then cells were perfused with the saturating Ca^{2+} solution. At the end of this procedure, 5 mM $MnCl_2$ was added to the bath to quench the fluorescence of the dye and determine the background values.

Confocal Microscopy. Fluorescence image (512 \times 512 \times 12 bit) acquisition was performed by a multi-channel Leica TCS SP5 laser scanning confocal microscope, equipped with an Argon laser (458, 476, 488 and 514 nm excitation lines), a green HeNe laser (543 nm), a red HeNe laser (633 nm) and a pulsed Chameleon multiphoton laser. A planapochromatic oil immersion objective 63x/1.4 and a one Airy disk unit pinhole diameter were used. Light collection configuration was optimized according to the combination of chosen fluorochromes, selecting the spectral windows by the acousto-optic beam splitter of the Leica SP5 scanning head and

performing a sequential channel acquisition protocol to reject possible cross-talk artefacts between acquisition channels. The Leica "LAS AF" software package was used for image acquisition. The software package "Image J" (release 1.49c, Wayne Rasband, NIH, MD, USA) was used to analyze the fluorescence intensity time-decays.

Assay of Ca^{2+} ATPase activity. Ca^{2+} ATPase activity was determined on cell homogenate at 25°C, using an enzyme-coupled spectrophotometric assay, in which hydrolysis of ATP is coupled to the oxidation of NADH. The NADH oxidation was followed at 340 nm. The assay medium contained: 100 mM Tris HCl pH 7.4, 2 mM $MgCl_2$, 150 mM $CaCl_2$, 50 mM KCl, 1 mM ATP, 0.15 mM phosphoenolpyruvate, 0.15 mM NADH, 10 units/ml lactate dehydrogenase, 5 units/ml pyruvate kinase. The assay was started with the addition of 15 μ g of the sample¹⁹. 3 μ M thapsigargin was employed to inhibit the Ca^{2+} ATPase activity.

Statistical analysis. Data were analyzed by one-way ANOVA and unpaired two-tail Student's t test using InStat software (GraphPad Software, Inc., La Jolla, CA, USA). Data are expressed as mean \pm standard deviation (SD) from 3 to 5 independent determinations performed in duplicate. In the figures SD are shown as error bars. An error probability with $P < 0.05$ was selected as significant.

1. Bagby, G. C. Genetic basis of Fanconi anemia. *Curr. Opin. Hematol.* **10**, 68–76 (2003).
2. Dufour, C. *et al.* TNF-alpha and IFN-gamma are overexpressed in the bone marrow of Fanconi anemia patients and TNF-alpha suppresses erythropoiesis in vitro. *Blood* **102**, 2053–2059 (2003).
3. Korthof, E. T. *et al.* Immunological profile of Fanconi anemia: a multicentric retrospective analysis of 61 patients. *Am. J. Hematol.* **88**, 472–476 (2013).
4. Pagano, G. *et al.* Oxidative stress as a multiple effector in Fanconi anaemia clinical phenotype. *Eur. J. Haematol.* **75**, 93–100 (2005).
5. Seif, A. E. Pediatric leukemia predisposition syndromes: clues to understanding leukemogenesis. *Cancer Genet.* **204**, 227–244 (2011).
6. Ravera, S. *et al.* Mitochondrial respiratory chain Complex I defects in Fanconi anemia complementation group A. *Biochimie* **95**, 1828–1837 (2013).
7. Capanni, C. *et al.* Changes in vimentin, lamin A/C and mitofilin induce aberrant cell organization in fibroblasts from Fanconi anemia complementation group A (FA-A) patients. *Biochimie* **95**, 1838–47 (2013).
8. Berridge, M. J., Lipp, P. & Bootman, M. D. The versatility and universality of Ca^{2+} signaling. *Nat. Rev. Mol. Cell. Biol.* **1**, 11–21 (2000).
9. Parekh, A. B. Store-operated CRAC channels: function in health and disease. *Nat. Rev. Drug Discov.* **9**, 399–410 (2010).



10. Sancak, Y. *et al.* EMRE is an essential component of the mitochondrial calcium uniporter complex. *Science* **342**, 1379–1382 (2013).
11. Gilabert, J. A. & Parekh, A. B. Respiring mitochondria determine the pattern of activation and inactivation of the store-operated Ca²⁺ current ICRAc. *EMBO J.* **19**, 6401–6407 (2000).
12. Gilabert, J. A., Bakowski, D. & Parekh, A. B. Energized mitochondria increase the dynamic range over which inositol 1,4,5-trisphosphate activates store-operated Ca²⁺ influx. *EMBO J.* **20**, 2672–2679 (2001).
13. Patergnani, S. *et al.* Calcium signaling around Mitochondria Associated Membranes (MAMs). *Cell Commun. Signal.* **9**, 19 (2011).
14. Glancy, B. & Balaban, R. S. Role of mitochondrial Ca²⁺ in the regulation of cellular energetics. *Biochemistry* **51**, 2959–2973 (2012).
15. Viola, H. M. & Hool, L. C. How does Ca²⁺ regulate mitochondrial energetics in the heart? - new insights. *Heart Lung Circ.* **23**, 602–609 (2014).
16. Duchen, M. R. Mitochondria and Ca²⁺ in cell physiology and pathophysiology. *Cell Calcium* **28**, 339–348 (2000).
17. Rao, W. *et al.* Blockade of SOCE protects HT22 cells from hydrogen peroxide-induced apoptosis. *Biochem. Biophys. Res. Commun.* **441**, 351–356 (2013).
18. Grynkiewicz, G., Poenie, M. & Tsien, R. Y. A new generation of Ca²⁺ indicators with greatly improved fluorescence properties. *J. Biol. Chem.* **260**, 3440–3450 (1985).
19. Panfoli, I., Morelli, A. & Pepe, I. M. Calcium pump in the disk membranes isolated from bovine retinal rod outer segments. *J. Photochem. Photobiol.* **24** (1994) 187–194.
20. Davidson, S. M. & Duchen, M. R. Imaging mitochondrial Ca²⁺ signalling with fluorescent probes and single or two photon confocal microscopy. *Methods Mol. Biol.* **810**, 219–234 (2012).
21. Ciarcia, R. *et al.* Dysregulated Ca²⁺ homeostasis and oxidative stress in chronic myeloid leukemia (CML) cells. *J. Cell. Physiol.* **224**, 443–453 (2010).
22. Revankar, C. M., Advani, S. H. & Naik, N. R. Altered Ca²⁺ homeostasis in polymorphonuclear leukocytes from chronic myeloid leukaemia patients. *Mol. Cancer* **5**, 65 (2006).
23. Rada, B. K. *et al.* Calcium signaling is altered in myeloid cells with a deficiency in NADPH oxidase activity. *Clin. Exp. Immunol.* **132**, 53–60 (2003).
24. Rizzuto, R. & Pozzan, T. Microdomains of intracellular Ca²⁺: molecular determinants and functional consequences. *Physiol. Rev.* **86**, 369–408 (2006).
25. Brookes, P. S. *et al.* Ca²⁺, ATP, and ROS: a mitochondrial love-hate triangle. *Am. J. Physiol. Cell. Physiol.* **287**, C817–C833 (2004).
26. Kumari, U., Ya Jun, W., Huat Bay, B. & Lyakhovich, A. Evidence of mitochondrial dysfunction and impaired ROS detoxifying machinery in Fanconi anemia cells. *Oncogene* **33**, 165–172 (2013).
27. Columbaro, M. *et al.* Treatment of FANCA cells with Resveratrol and N-Acetylcysteine: A comparative study. *Plos One* (2014) doi: 10.1371/journal.pone.0104857. eCollection 2014.
28. Cuccarolo, P., Viaggi, S. & Degan, P. New insights into redox response modulation in Fanconi's anemia cells by hydrogen peroxide and glutathione depletors. *FEBS J.* **279**, 2479–2494 (2012).
29. Ravera, S. *et al.* Inhibition of metalloproteinase activity in FANCA is linked to altered oxygen metabolism. *J. Cell. Physiol.* (2014) doi: 10.1002/jcp.24778.
30. Cappelli, E. *et al.* Mitochondrial respiratory complex I defects in Fanconi anemia. *Trends Mol. Med.* **19**, 513–514 (2013).
31. Ishihara, N., Fujita, Y., Oka, T. & Mihara, K. Regulation of mitochondrial morphology through proteolytic cleavage of OPA1. *EMBO J.* **25**, 2966–2977 (2006).
32. McBride, H. & Soubannier, V. Mitochondrial function: OMA1 and OPA1, the grandmasters of mitochondrial health. *Curr. Biol.* **20**, R274–R276 (2010).
33. Kushnareva, Y. E. *et al.* Loss of OPA1 disturbs cellular Ca²⁺ homeostasis and sensitizes for excitotoxicity. *Cell Death Differ.* **20**, 353–365 (2013).
34. Head, B. *et al.* Inducible proteolytic inactivation of OPA1 mediated by the OMA1 protease in mammalian cells. *J. Cell Biol.* **187**, 959–966 (2009).
35. Ehse, S. *et al.* Regulation of OPA1 processing and mitochondrial fusion by m-AAA protease isoenzymes and OMA1. *J. Cell Biol.* **187**, 1023–1036 (2009).
36. MacVicar, T. D. & Lane, Y. D. Impaired OMA1-dependent cleavage of OPA1 and reduced DRP1 fission activity combine to prevent mitophagy in cells that are dependent on oxidative phosphorylation. *J. Cell Sci.* **127**, 2313–2325 (2014).
37. Marzec, M., Eletto, D. & Argon, Y. GRP94: An HSP90-like protein specialized for protein folding and quality control in the endoplasmic reticulum. *Biochim. Biophys. Acta* **1823**, 774–787 (2012).
38. Oakes, S. A., Lin, S. S. & Bassik, M. C. The control of endoplasmic reticulum-initiated apoptosis by the BCL-2 family of proteins. *Curr. Mol. Med.* **6**, 99–109 (2006).
39. van Vliet, A. R., Verfaillie, T. & Agostinis, P. New functions of mitochondria associated membranes in cellular signaling. *Biochim. Biophys. Acta* **1843**, 2253–2262 (2014).
40. Hetz, C. & Glimcher, L. The daily job of night killers: alternative roles of the BCL-2 family in organelle physiology. *Trends Cell. Biol.* **18**, 38–44 (2008).
41. Minagawa, N. *et al.* The anti-apoptotic protein Mcl-1 inhibits mitochondrial Ca²⁺ signals. *J. Biol. Chem.* **280**, 33637–33644 (2005).
42. Greenberg, E. F., Lavik, A. R. & Distelhorst, C. W. Bcl-2 regulation of the inositol 1,4,5-trisphosphate receptor and calcium signaling in normal and malignant lymphocytes: Potential new target for cancer treatment. *Biochim. Biophys. Acta* **1843**, 2205–2210 (2014).
43. Bánsághi, S. *et al.* Isoform- and species-specific control of inositol 1,4,5-trisphosphate (IP₃) receptors by reactive oxygen species. *J. Biol. Chem.* **289**, 8170–81 (2014).
44. Rada, B. K., Geiszt, M., Hably, C. & Ligeti, E. Consequences of the electrogenic function of the phagocytic NADPH oxidase. *Philos. Trans. R. Soc. Lond. B. Biol. Sci.* **360**, 2293–2300 (2005).
45. Li, Q. *et al.* Endosomal Nox2 facilitates redox-dependent induction of NF-κB by TNF-α. *Antioxid. Redox Signal.* **11**, 1249–1263 (2009).
46. Huang, Y. *et al.* TNF-α induces endothelial dysfunction via PKC-ζ-dependent NADPH oxidase activation. *J. Huazhong Univ. Sci. Technol. Med. Sci.* **32**, 642–647 (2012).
47. Moe, K. T. *et al.* Tumor necrosis factor-α-induced nuclear factor-κB activation in human cardiomyocytes is mediated by NADPH oxidase. *J. Physiol. Biochem.* (2014) Jul 25 [Epub ahead of print].
48. McCalley, A. E., Kaja, S., Payne, A. J. & Koulen, P. Resveratrol and Ca²⁺ signaling: molecular mechanisms and clinical relevance. *Molecules* **19**, 7327–7340 (2014).
49. Csiszar, A. Anti-inflammatory effects of resveratrol: possible role in prevention of age-related cardiovascular disease. *Ann. N. Y. Acad. Sci.* **1215**, 117–122 (2011).
50. Sareen, D., Darjatmoko, S. R., Albert, D. M. & Polans, A. S. Mitochondria, calcium, and calpain are key mediators of resveratrol-induced apoptosis in breast cancer. *Mol. Pharmacol.* **72**, 1466–1475 (2007).
51. Sassi, N. *et al.* Mitochondria-targeted resveratrol derivatives act as cytotoxic pro-oxidants. *Curr. Pharm. Des.* **20**, 172–179 (2014).

Acknowledgments

The samples were obtained from the “Cell Line and DNA Biobank from Patients affected by Genetic Diseases” (G. Gaslini Institute) - Telethon Genetic Biobank Network (Project No. GTB07001). We do acknowledge Fondi 5 per mille IRCCS AOU San Martino - IST, AIRFA, ERG spa, Cambiaso & Risso, Rimorchiatori Riuniti, Saar Depositi Oleari Portuali, UC Sampdoria for supporting the activity of the Clinical & Experimental Hematology Unit of G. Gaslini Institute and of SC Mutagenesis, IRCCS AOU San Martino - IST.

Author contributions

C.U.: experimental work with fluorimetric and confocal microscopy; SR: Exp. Biochemistry; P.C.: Cell Lab management; I.P.: Exp. Biochemistry, Discussion, Authorship support; C.D.: Clinician, Lab management; E.C.: Exp. Design, MS Authorship; P.D.: Exp. Design, MS Authorship.

Additional information

Competing financial interests: The authors declare no competing financial interests.

How to cite this article: Usai, C. *et al.* Dysregulated Ca²⁺ Homeostasis in Fanconi anemia cells. *Sci. Rep.* **5**, 8088; DOI:10.1038/srep08088 (2015).



This work is licensed under a Creative Commons Attribution-NonCommercial-NoDerivs 4.0 International License. The images or other third party material in this article are included in the article's Creative Commons license, unless indicated otherwise in the credit line; if the material is not included under the Creative Commons license, users will need to obtain permission from the license holder in order to reproduce the material. To view a copy of this license, visit <http://creativecommons.org/licenses/by-nc-nd/4.0/>